2024 European Control Conference (ECC)
June 25-28, 2024. Stockholm, Sweden

Control of Underactuated Autonomous Underwater Vehicles With Input Saturation Based on Passivity Using Feedback Concavification

Shuyuan Fan and Herbert Werner

Abstract— **This paper proposes a concept of feedback concavification to the control of an underactuated autonomous underwater vehicle (AUV) with 6-DOF, subject to actuator saturation, to improve transient performance and robustness, taking into account the presence of unknown model dynamics and disturbances. To address the underactuated problem under the dissipation framework, Euclidean geometry is utilized to match the dimensions of the input and output. Therefore, an interconnected architecture for the AUV system is proposed, enabling the AUV system to be transformed into interconnected passive systems via feedback within this architecture with guaranteed asymptotic stability. The concave passivity is then applied to the interconnected passive systems to handle uncertainties, disturbances, and actuator saturation problems. The proposed method with assigned concavity is effective in different scenarios with fast transient response and the decreasing L_2-gain under actuator saturation. Numerical simulations have demonstrated the effectiveness of the proposed interconnected passive architecture and the feedback concavification approach in improving the control performance of the underactuated AUV.**

I. INTRODUCTION

The underactuated AUV is a typical and highly used underactuated system. Underactuated AUVs are more widely used in practical applications because of the low energy consumption, cost, and weight compared to fully actuated AUVs and over-actuated AUVs [1]. The control of underactuated AUVs is still a challenging problem due to the presence of external disturbances, model uncertainties, coupling nonlinearities, underactuated characteristics and actuators' constraints (See [2]–[10] for the details). To address these issues, it's crucial to design a highly robust controller for AUV systems. Those research tend to opt for simplified numerical models such as 3-DOF, 4-DOF, and 5-DOF configurations. Nevertheless, it is crucial to emphasize that the complete 6-DOF dynamic model holds significant importance and offers a broader perspective in the field of AUVs [5]. Extending the control methods from the lower-DOF model to the higher-DOF model is tough. On the contrary, the control methods for 6-DOF model can be easily extended to the lower-DOF model by enforcing some states to be zero. For this purpose, this paper focuses on the underactuated 6-DOF dynamic model of a realistic mini-AUV developed and identified by TUHH [11]. There is some research on this model as shown in [12]–[14], where a PD controller is deployed, but without incorporating considerations for robustness. With that PD controller, it is difficult to take the other tough tasks [12]–[14], e.g. tracking different kinds of references with different velocities or amplitudes. This motivates the authors to design a robust controller with multiple functions.

Shuyuan Fan is with the Institute of Control Systems, Hamburg University of Technology, Eissendorfer Str. 40, 21073 Hamburg, Germany shuyuan.fan@tuhh.de

Herbert Werner is with the Institute of Control Systems, Hamburg University of Technology, Eissendorfer Str. 40, 21073 Hamburg, Germany h.werner@tuhh.de

The control system always requires the total energy to be dissipative to guarantee stability and control performance. Dissipation inequalities introduced by Willems in [15] are widely used for the analysis and design of interconnected nonlinear systems, particularly the passive system with the quadratic supply rate which is always utilized to guarantee the stability and robustness (L_2-gain), and the related theorem and techniques are fairly mature (See [16]–[18] for the details). Dissipativity describes input-output properties, and the associated supply rate is a one-dimensional map from input and output to the real number. Though the definition of a dissipative system does not explicitly require input and output to have the same dimensions, it is generally assumed when designing interconnected passive systems with quadratic supply rate, as presented in [18], [19]. However, due to the underactuated properties, the input dimension and the output (interconnection) dimension do not match. Thankfully, the Euclidean vector provides a way to transform a 3D vector into a one-dimensional vector together with a direction vector, which enables the underactuated AUV to unify the dimensions of input and output (interconnection). This inspired the authors to develop an interconnected passive architecture for underactuated AUVs. In addition, for the existing framework of the passive system, assigning a globally desired L_2-gain requires sufficient actuator's efforts, which cannot be satisfied due to the actuator's saturation. Thus, to enhance the robustness and transient response within the actuators' saturation, the feedback concavification idea is introduced to the passive system with a decreasing L_2-gain towards to the desired convergence equilibrium by using the proposed concave factor.

This paper offers two notable contributions. Firstly, it defines an interconnected passive structure for AUVs utilizing Euclidean vectors. Within this framework, it becomes straightforward to allocate and design performance (L_2-gain) through the feedback methods. Secondly, it introduces feedback concavification techniques to tackle issues arising from uncertainties, disturbances, and actuator saturation. It is important to emphasize that concavity is determined in relation to the Lyapunov function or storage function rather than the system states.

$Notation$: Throughout this paper, the set $\mathbb{R}$, $\mathbb{R}_+$, and $\mathbb{R}_{\geq 0}$ denote the set of real numbers, positive real numbers, and

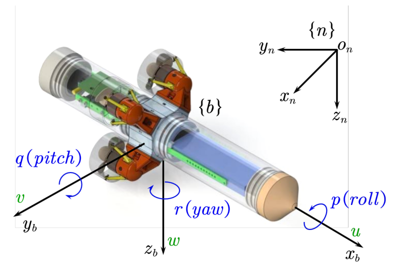

Fig. 1. 6 DOF velocities u, v, w, p, q and r in the body-fixed frame $\{b\}$ of the Hippocampus and inertial reference frame $\{n\}$

non-negative real numbers, respectively. $\mathbb{R}^n$ denotes the n-dimensional Euclidean space. $||\cdot||$ denotes the Euclidean norms. $\lambda_{(\cdot)}$ denotes the eigenvalues of a square matrix $(\cdot)$. $\bar{\lambda}_{(\cdot)}$ and $\underline{\lambda}_{(\cdot)}$ denote the maximum and minimum eigenvalue of a square matrix $(\cdot)$, respectively. $M \prec (\succ) 0$ implies M is negative (positive) definite. $\dot{V} = \frac{\mathrm{d}V}{\mathrm{d}t}$. The set of real-valued square-integrable signals $u : [0, \infty) \to \mathbb{R}^m$ is denoted by $\mathcal{L}_2^m[0, \infty)$, with $\mathcal{L}_{2e}[0, \infty)$ denoting the associated extended signal space [18]. For a vector $\nu \in \mathbb{R}^3$, $\nu^* \in \mathbb{R}$ denotes the Euclidean distance by the notation *. For a Euclidean vector $\vec{a} := [a_1, a_2, a_3]^\top \in \mathbb{R}^3$, then define

$$\vec{a} = ||\vec{a}||\Gamma(\theta_a, \psi_a) = \vec{a}^*\Gamma(\theta_a, \psi_a)$$
$$\Gamma(\theta_a, \psi_a) := \begin{bmatrix} \cos(\theta_a)\cos(\psi_a) \\ \cos(\theta_a)\sin(\psi_a) \\ -\sin(\psi_a) \end{bmatrix}$$

where $\theta_a := \operatorname{atan2}(-a_2, \sqrt{a_1^2 + a_2^2}), \psi_a := \operatorname{atan2}(a_2, a_1)$.

II. Underactuated AUV and Problem Formulation

A. Underactuated AUV Modeling

This paper considers the *Hippocampus*, an autonomous underwater vehicle developed at TUHH [11] with actuator saturation (See Fig.1). The 6-DOF mathematical representation of the AUV is derived and characterized in reference to [11], drawing from the well-known handbook on underwater vehicles [3]. It can be expressed as follows:

$$\Sigma : \begin{cases} \dot{\eta} = J(\Theta)\boldsymbol{v} \\ M\dot{v} = -C(\boldsymbol{v})\boldsymbol{v} - D(\boldsymbol{v})\boldsymbol{v} - g(\eta) + \tau_d + \tau \end{cases} \quad (1)$$

with $\eta = [\begin{array}{cc} X^\top & \Theta^\top \end{array}]^\top \in \mathbb{R}^6$, $\boldsymbol{v} = [\begin{array}{cc} \nu^\top & \omega^\top \end{array}]^\top \in \mathbb{R}^6$, where $X = [\begin{array}{ccc} x & y & z \end{array}]^\top$ is the position vector which represents the distance from the inertial frame $\{n\}$ to the body fixed frame $\{b\}$, expressed in NED coordinates (See Fig.1), $\Theta = [\begin{array}{ccc} \phi & \theta & \psi \end{array}]^\top$ is the orientation vector which denotes the three Euler angles in three-dimensional space, $\nu = [\begin{array}{ccc} u & v & w \end{array}]^\top$ describes the linear velocity, and $\omega = [\begin{array}{ccc} p & q & r \end{array}]^\top$ denotes the angular velocity. $\tau_d \in \mathbb{R}^6$ denotes the uncertainties and disturbance and $\boldsymbol{\tau} = [\begin{array}{cccccc} f & 0 & 0 & \tau_{roll} & \tau_{pitch} & \tau_{yaw} \end{array}]^\top$ denotes the control input vector with underactuated property, which includes the thrust force f and three moments $\tau_{roll}, \tau_{pitch}, \tau_{yaw}$. Define $\tau_s := [\begin{array}{cccc} f & \tau_{roll} & \tau_{pitch} & \tau_{yaw} \end{array}]^\top$, where τ_s satisfies the saturation $\tau_s = L\mathrm{Sat}(\mathcal{T})$ with $\mathcal{T} \in \mathbb{R}^4$ is the torque vector of four deployed motors, and L is a matrix map from the torque vector to the input vector τ_s. $\boldsymbol{J}(\boldsymbol{\eta}) = \mathrm{diag}(R(\boldsymbol{\Theta}), T(\boldsymbol{\Theta}))$ is the block diagonal matrix consisting of the linear velocity transformation matrix $R(\boldsymbol{\Theta})$ between $\{b\}$ and $\{n\}$, and the angular velocity transformation matrix $T(\boldsymbol{\Theta})$. $M \in \mathbb{R}^{6\times6}$ represents the combined mass matrix, $C(\boldsymbol{v}) \in \mathbb{R}^{6\times6}$ represents the matrix of Coriolis effects, $D(\boldsymbol{v}) \in \mathbb{R}^{6\times6}$ is the hydrodynamic damping matrix, and $g(\eta) \in \mathbb{R}^6$ describes the hydrostatic load for a neutrally buoyant underwater vehicle. Those values are identified by [20].

B. Problem Formulation

Assume the underactuated AUV can reach and track an admissible position reference trajectory $X_{ref}(t) : \mathbb{R}_{\geq 0} \to \mathbb{R}^3$ starting from any admissible initial position states $X(0)$. The maximum velocity of the AUV model is constrained by the actuator saturation. Thus, the comprehensive velocity of $X_{ref}(t)$ should within this constraint. Considering the numerical dynamic model (1) with the unknown disturbance τ_d, design τ under the input saturation so that the underactuated AUV can converge to the reference trajectory such that

$$\lim_{t\to\infty} \|X(t) - X_{ref}(t)\| \leq \delta \quad (2)$$

where δ is positive and arbitrarily small.

III. Concave Passive Systems

This section presents the formulation of a concave passive system with the help of the concave factor and concave factor matrix. As a reminder, we uses separate notations in this section.

A. Concave Factors and Concave Factor Matrices

Firstly, we introduce the definition of a concave factor.

Definition 1 (Concave factor)**.** *For a smooth concave function $F(\rho) = f_c(\rho)\rho$, where $f(\rho) : \mathbb{R}_{\geq 0} \to \mathbb{R}_+$ is bounded and smooth for $\rho \in [0, \infty)$, $f(\rho)$ is called a concave factor with respect to ρ, and we have $\frac{\mathrm{d}}{\mathrm{d}\rho} f_c(\rho) < 0$.*

The concave factor can be considered as the 'gain' which increases as ρ decreases. This paper will utilize the properties of the concave factor. Here we propose a slider-like concave factor function, such that

$$f_c(\rho) = \frac{\beta_1 k_{min}\rho^\alpha + \beta_2 k_{max}}{\beta_1\rho^\alpha + \beta_2} \quad (\beta_1, \beta_2 > 0, 0 < \alpha \leq 1)$$

where the low gain k_{min} is selected to address the input saturation, a larger control gain k_{max} to ensure the performance, and β_1, β_2 can shift the sliding speed from k_{min} to k_{max} with the decrease of ρ. Then, we extend it to the vector space as the concave factor matrix.

Definition 2 (Concave factor matrix for quadratic function)**.** *For a quadratic convex function $V = x^\top Px$ with $x \in \mathbb{R}^n$ and $P \succ 0$, if and only if $F(x) := x^\top M(x)x$ is concave with respect to V with $M(x) \succ 0$, $M(x)$ is called a concave factor matrix with respect to the quadratic convex function V for the vector x, which satisfies $\frac{\mathrm{d}}{\mathrm{d}V} M(x) \prec 0$.*

B. Concave Passivity

Now, we introduce the concave passive system with the help of the concave factor matrix. Consider the continuous-time nonlinear system as follows

$$\Sigma_p : \begin{cases} \dot{x} = f(x,u) \\ y = h(x) \end{cases} \tag{3}$$

with state $x \in \mathcal{X} \subseteq \mathbb{R}^n$, input $u \in \mathcal{U} \subseteq \mathbb{R}^m$ and output $y \in \mathcal{Y} \subseteq \mathbb{R}^m$. The maps f and h are assumed to be sufficiently smooth and all input functions $u(\cdot), y(\cdot) \in \mathcal{L}_{2e}^m[0,\infty)$. The system is assumed to be fully controllable for all $x \in \mathcal{X}$. Moreover, we assume $f(0,0) = 0$ and $h(0) = 0$, such that $(u_e, x_e, y_e) = (0,0,0)$ is an equilibrium. We propose the concave output strictly passive system based on the passivity presented in [18].

Definition 3 (Concave output strictly passive system)**.** *For a system as Σ_p, suppose it is dissipative with respect to the supply rate $s(u,y) := u^\top Sy - y^\top Q(x)y$ with a non-negative convex storage function V, where $s : \mathcal{U} \times \mathcal{Y} \to \mathbb{R}$ and $V : \mathcal{X} \to \mathbb{R}_{\geq 0}$, and u and y have the same dimensions. System Σ_p is called a concave output strictly passive system if $Q(x) \succ 0$ is a concave factor matrix with respect to the storage function V (V has the quadratic form) for the vector y that $\frac{\mathrm{d}(Q(x))}{\mathrm{d}V} \prec 0$.*

In the above definition, if $Q(x)$ is a constant matrix that $\frac{\mathrm{d}(Q(x))}{\mathrm{d}V} \equiv 0$, then system Σ_p is called a output strictly passive system.

C. Benefits of the Concave Output Strictly Passive System

The concave output strictly passive system is proposed to improve the robustness and convergence rate under the input saturation. Now, we analyze its robustness represented by L_2-gain.

Proposition 1. *Σ_p has the L_2-gain $G(y,u) \leq \frac{\sqrt{\bar{\lambda}_{SS^\top}}}{\underline{\lambda}_{Q(x)}}$ if it is concave output strictly passive.*

Proof: Based on the definition, for the concave output strictly passive system, we have the dissipation inequality

$$\begin{aligned} \frac{\mathrm{d}}{\mathrm{d}t}V(x) &\leq u^\top Sy - y^\top Q(x)y \leq u^\top Sy - \underline{\lambda}_{Q(x)}||y||^2 \\ &\leq u^\top Sy - \underline{\lambda}_{Q(x)}||y||^2 + \left\| \sqrt{\frac{1}{2\underline{\lambda}_{Q(x)}}}S^\top u - \sqrt{\frac{\underline{\lambda}_{Q(x)}}{2}}y \right\|^2 \\ &\leq \frac{\bar{\lambda}_{SS^\top}}{2\underline{\lambda}_{Q(x)}}||u||^2 - \frac{1}{2}\underline{\lambda}_{Q(x)}||y||^2 \\ &= \frac{\underline{\lambda}_{Q(x)}}{2}\left(\left(\frac{\sqrt{\bar{\lambda}_{SS^\top}}}{\underline{\lambda}_{Q(x)}} \right)^2 ||u||^2 - ||y||^2 \right) \end{aligned}$$

which implies Σ_p has the L_2-gain $G(y,u) \leq \frac{\sqrt{\bar{\lambda}_{SS^\top}}}{\underline{\lambda}_{Q(x)}}$ which is similar to the relevant proof presented in [18].

Due to the concavity, we obtain $\frac{\mathrm{d}}{\mathrm{d}V}\left(\frac{\sqrt{\bar{\lambda}_{SS^\top}}}{\underline{\lambda}_{Q(x)}} \right) > 0$. This implies for the concave output strictly passive system, its L_2-gain decreases as V decreases, such that the robustness is enhanced towards to the convergence equilibrium.

Generally, u in system Σ_p is considered as the external disturbance. Thus, we can evaluate the convergence performance with the dissipation inequality by assuming $u \equiv 0$. Therefore, we have

$$\frac{\mathrm{d}}{\mathrm{d}t}V(x) \leq -y^\top Q(x)y \tag{4}$$

Suppose $V(x) = y^\top \hat{M}y$ with $\hat{M} \succ 0$. Then, we have

$$\frac{\mathrm{d}}{\mathrm{d}t}V(x) \leq -\frac{\underline{\lambda}_{Q(x)}}{\bar{\lambda}_{\hat{M}}}V(x), \quad V_0 = V(x(0)) \tag{5}$$

Therefore, $V(x(t)) \leq e^{-\frac{\underline{\lambda}_{Q(x)}}{\bar{\lambda}_{\hat{M}}}t}V_0$. This implies the convergence rate increases as V decreases.

IV. Controller Design by Feedback

This section, we design the feedback control law with the concave passivity. To assign the desired passivity in the underwater vehicle, an interconnected architecture for AUV is proposed with four subsystems.

A. An Interconnected Architecture for AUV With the Reduced Dimension

Without any simplification, we can split the whole system Σ into four subsystems, such that

$$\Sigma_1 : \begin{cases} \dot{X} = R(\Theta)\nu \\ y_1 = h_1(X) \end{cases}$$

$$\Sigma_2 : \begin{cases} M_1\dot{\nu} = -C_1(\nu)\omega - D_1(\nu)\nu - g_1(\eta) + \tau_{d1} + \tau_1 \\ y_2 = h_2(\nu) \end{cases}$$

$$\Sigma_3 : \begin{cases} \dot{\Theta} = T(\Theta)\omega \\ y_3 = h_3(\Theta) \end{cases}$$

$$\Sigma_4 : \begin{cases} M_2\dot{\omega} = -C_1(\nu)\nu - C_2(\omega)\omega - D_2(\omega)\omega - g_2(\eta) + \tau_{d2} + \tau_2 \\ y_4 = h_4(\omega) \end{cases}$$

where

$$C(\upsilon) = \begin{bmatrix} 0_{3\times3} & C_1(\nu) \\ C_1(\nu) & C_2(\omega) \end{bmatrix} \quad D(\upsilon) = \begin{bmatrix} D_1(\nu) & 0_{3\times3} \\ 0_{3\times3} & D_2(\omega) \end{bmatrix}$$

where $C_1(\nu), C_2(\omega) \in \mathbb{R}^{3\times3}$ are skew-symmetric matrices, $M = \mathrm{diag}(M_1, M_2)$ with $M_1, M_2 \succ 0 \in \mathbb{R}^{3\times3}$, $g(\eta) = [g_1(\eta), g_2(\eta)]^\top$ with $g_1(\eta), g_2(\eta) \in \mathbb{R}^3$,$\tau_d = [\tau_{d_1}, \tau_{d_2}]^\top$ with $\tau_{d_1}, \tau_{d_2} \in \mathbb{R}^3$,$\tau_d = [\tau_1, \tau_2]^\top$ with $\tau_1, \tau_2 \in \mathbb{R}^3$. Due to the underactuated properties $\tau_1 = [f,0,0]^\top$, the dimension condition $y_2 \in \mathbb{R}$ should hold to assign a passive system. Moreover, the interconnection between Σ_1 and Σ_2 should be reduced to be one dimensional to match the size for assigning passive interconnected systems. Then, define

$$\nu := \Gamma(\theta_\nu, \psi_\nu)\nu^* \qquad \tau_{d_1} := \Gamma(\theta_{\tau_{d_1}}, \psi_{\tau_{d_1}})\tau_{d_1}^*$$

where $\nu^*, \tau_{d_1}^* \in \mathbb{R}$. Define the interconnection that $y_2 := \nu^*$, $y_3 := \Theta$, $y_4 := \omega$, then we can obtain an interconnected system as shown in Fig.2. Moreover, y_1 should be designed later.

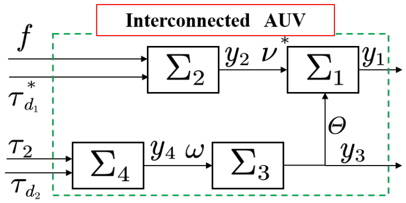

Fig. 2. The equivalent interconnected system

B. Passivity by Feedback

We transform the four interconnected subsystems $\Sigma_1, \Sigma_2, \Sigma_3, \Sigma_4$ into four passive interconnected subsystems denoted by $\Sigma_1^p, \Sigma_2^p, \Sigma_3^p, \Sigma_4^p$ by feedback. The designed equivalent passive interconnected system is shown as Fig.3 with the associated connections $\hat{u}_1 = \hat{y}_2$ and $\hat{u_3} = \hat{y_4}$, where the other parameters will be introduced later. Each passive subsystem Σ_i^p $(i = \{1,2,3,4\})$ is dissipative with respect to the supply rate $s_i(\hat{u}_i, \hat{y}_i) := \hat{u}_i^\top S_i \hat{y}_i - \hat{y}_i^\top Q_i \hat{y}_i$ with the storage function V_i, where $Q_i \succ 0$. The key is to find suitable $\hat{u}_i, \hat{y}_i, S_i, Q_i, V_i$ where Q_i is the parameter to be tuned for obtaining the desired control performance.

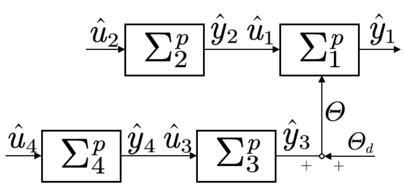

Fig. 3. The equivalent passive interconnected system

1) Passivity for Σ_1: We design: $V_1 := \frac{1}{2}\|X - X_{ref}\|^2$, $\hat{y}_1 := \Gamma^\top(\theta_\nu, \psi_\nu) R^\top(\Theta)(X - X_{ref})$, $\hat{u}_1 := \nu^* + Q_1\hat{y}_1 + \nu_{ref}^* S_{ref}$, where

$$
\begin{aligned}
S_{ref} &= -\Gamma^\top(\theta_{\nu_{ref}}, \psi_{\nu_{ref}}) R(\Theta) \hat{\Gamma}_\nu^{-\top} \Gamma(\theta_\nu, \psi_\nu) \\
\nu_{ref} &= \dot{X}_{ref}, \quad \hat{\Gamma}_\nu := \Gamma(\theta_\nu, \psi_\nu)\Gamma^\top(\theta_\nu, \psi_\nu).
\end{aligned}
$$

Thus, we have

$$
\begin{aligned}
\dot{V}_1 &= \left(R(\Theta)\nu - \dot{X}_{ref}\right)^\top (X - X_{ref}) \\
&= \left(\nu^* \Gamma^\top(\theta_\nu, \psi_\nu) R^\top(\Theta) - \nu_{ref}^\top\right)(X - X_{ref}) \\
&= \hat{u}_1 \hat{y}_1 - Q_1 \hat{y}_1^2
\end{aligned}
\tag{6}
$$

Hence, $S_1 = 1$ and the designed $\hat{u}_1, \hat{y}_1$ can formulate a output strictly passive system Σ_1^p.

2) Passivity for Σ_2: Let $\nu_f^* := Q_1\hat{y}_1 + \nu_{ref}^* S_{ref}$. Design $\hat{u}_2 := \tau_{d_1}^*$, $V_2 := \frac{1}{2}\hat{y}_2 \Gamma^\top(\theta_\nu, \psi_\nu) M_1 M_1 \Gamma(\theta_\nu, \psi_\nu)\hat{y}_2$. Thus,

$$
\begin{aligned}
\dot{V}_2 = &\underbrace{(-C_1(\nu)\omega - D_1(\nu)\nu - g_1(\eta) - \frac{\mathrm{d}M_1\Gamma(\theta_\nu, \psi_\nu)\nu_f^*}{\mathrm{d}t}}_{H} \\
&+ \hat{u}_2 \Gamma(\theta_{\tau_{d_1}}, \psi_{\tau_{d_1}}) + f\Gamma(0,0))^\top M_1 \Gamma(\theta_\nu, \psi_\nu)\hat{y}_2 \\
= &(H^\top + f\Gamma^\top(0,0)) M_1 \Gamma(\theta_\nu, \psi_\nu)\hat{y}_2 + \hat{u}_2 S_2 \hat{y}_2
\end{aligned}
$$

with $S_2 = \Gamma^\top(\theta_{\tau_{d_1}}, \psi_{\tau_{d_1}}) M_1 \Gamma(\theta_\nu, \psi_\nu)$. Then, define

$$
(H^\top + f\Gamma^\top(0,0)) M_1 \Gamma(\theta_\nu, \psi_\nu) = -Q_2 \hat{y}_2 \tag{7}
$$

Solving equation (7), we obtain the solution

$$
f = -\frac{Q_2\hat{y}_2 + H^\top M_1 \Gamma(\theta_\nu, \psi_\nu)}{\Gamma^\top(0,0) M_1 \Gamma(\theta_\nu, \psi_\nu)} \quad (\cos(\theta_\nu)\cos(\psi_\nu) \neq 0) \tag{8}
$$

Clearly, $\cos(\theta_\nu)\cos(\psi_\nu) = 0$ if and only if $u = 0, v^2 + w^2 \neq 0$. Generally speaking, $-\frac{\pi}{4} \leq \theta_\nu, \psi_\nu \leq \frac{\pi}{4}$ due to v, w come from the Coriolis effect.

3) Passivity for Σ_3: Although Σ_1^p is output strictly passive, the asymptotic stability can not be guaranteed, which is related to the configuration of Θ. Assume the configuration Θ_d is sufficient to achieve the asymptotic stability and $\Theta_d = 0$ when $X = X_{ref}$. Design $\hat{y}_3 := y_3 - \Theta_d$, $V_3 := \frac{1}{2}\hat{y}_3^\top \hat{y}_3$, $S_3 := T^\top(\Theta)$, and $\hat{u}_3 := \omega - \omega_f$ where $\omega_f := T^{-1}(\Theta)\left(-Q_3\hat{y}_3 + \dot{\Theta}_d\right)$. Therefore,

$$
\begin{aligned}
\dot{V}_3 &= \hat{u}_3^\top T^\top(\Theta)\hat{y}_3 + \omega_f^\top T^\top(\Theta)\hat{y}_3 - \dot{\Theta}_d^\top \hat{y}_3 \\
&= \hat{u}^\top S_3 \hat{y}_3 - \hat{y}_3^\top Q_3 \hat{y}_3
\end{aligned}
$$

This implies the designed parameters can lead to a passive system Σ_p^3.

4) Passivity for Σ_4: Design $V_4 := \frac{1}{2}\hat{y}_4 M_2 M_2 \hat{y}_4$, $\hat{u}_4 := \tau_{d_2}$, $S_4 := M_2$. Let $O := -C_1(\nu)\nu - C_2(\omega)\omega - D_2(\omega)\omega - g_2(\eta)$. Hence,

$$
\frac{\mathrm{d}}{\mathrm{d}t}V_4 = \hat{u}_4^\top M_2 \hat{y}_4 + \left(O^\top - \dot{w}_f^\top M_2 + \tau_2^\top\right) M_2 \hat{y}_4
$$

For obtaining a passive system, we design $M_2 O - M_2 M_2 \dot{\omega}_f + M_2 \tau_2 = -Q_4 \hat{y}_4$. Hence, we have

$$
\tau_2 = M_2^{-1}(-Q_4\hat{y}_4 - M_2 O + M_2 M_2 \dot{\omega}_f) \tag{9}
$$

Thus, we obtain the control law based on the passivity,

$$
\tau_s = \begin{bmatrix} f \\ \tau_2 \end{bmatrix} = \begin{bmatrix} -\frac{Q_2\hat{y}_2 + H^\top M_1 \Gamma(\theta_\nu, \psi_\nu)}{\Gamma^\top(0,0) M_1 \Gamma(\theta_\nu, \psi_\nu)} \\ M_2^{-1}(-Q_4\hat{y}_4 - M_2 O + M_2 M_2 \dot{\omega}_f) \end{bmatrix}. \tag{10}
$$

Consequently, we can assign the interconnected passive system as shown in Fig.3 by executing the control law (10). This system is output strictly passive with respect to the supply rate $s = s_1 + s_2 + s_3 + s_4$ with the storage function $V = V_1 + V_2 + V_3 + V_4$.

C. Stability analysis

1) Stability for $\tau_d \equiv 0$: For $\tau_d \equiv 0$, we have

$$
\dot{V} = \begin{bmatrix} \hat{y}_1 \\ \hat{y}_2 \end{bmatrix}^\top \begin{bmatrix} -Q_1 & \frac{S_1^\top}{2} \\ \frac{S_1}{2} & -Q_2 \end{bmatrix} \begin{bmatrix} \hat{y}_1 \\ \hat{y}_2 \end{bmatrix} + \begin{bmatrix} \hat{y}_3 \\ \hat{y}_4 \end{bmatrix}^\top \begin{bmatrix} -Q_3 & \frac{S_3^\top}{2} \\ \frac{S_3}{2} & -Q_4 \end{bmatrix} \begin{bmatrix} \hat{y}_3 \\ \hat{y}_4 \end{bmatrix}
$$

Define $Z := \begin{bmatrix} X_e^\top & \Theta^\top & \nu^\top & \omega^\top \end{bmatrix}^\top$ with $X_e := X - X_{ref}$, and $Y := \begin{bmatrix} \hat{y}_1 & \hat{y}_2 & \hat{y}_3^\top & \hat{y}_4^\top \end{bmatrix}^\top$. We can easily design the sufficient large Q_1, Q_2, Q_3, Q_4, such that

$$
\begin{bmatrix} -Q_1 & \frac{S_1^\top}{2} \\ \frac{S_1}{2} & -Q_2 \end{bmatrix} \prec 0, \quad \begin{bmatrix} -Q_3 & \frac{S_3^\top}{2} \\ \frac{S_3}{2} & -Q_4 \end{bmatrix} \prec 0. \tag{11}
$$

Proposition 2. *Suppose the condition (11) holds. The AUV is asymptotically stable at $Z = 0$, if $\Gamma^\top(\theta_\nu, \psi_\nu) R^\top(\Theta) \Gamma^\top(\theta_{X_e}, \psi_{X_e}) \neq 0$ holds $\forall Z \neq 0$.*

Proof: Since the inequality (11) holds, then we have $\lim_{t\to\infty} Y = 0$, such that $\lim_{t\to\infty} \hat{y}_i = 0 \quad (i = 1,2,3,4)$. Since

$\Gamma^\top(\theta_\nu,\psi_\nu)R^\top(\Theta)\Gamma^\top(\theta_{X_e},\psi_{X_e}) \neq 0$ holds $\forall Z \neq 0$, then $\hat{y}_1 = 0$ implies $X_e = 0$, such that $\Theta_d = 0$. Hence, $\lim_{t\to\infty}\Theta = 0$. Therefore, $\lim_{t\to\infty} Z = 0$. This completes the proof.

Thus, to avoid $\Gamma^\top(\theta_\nu,\psi_\nu)R^\top(\Theta)\Gamma^\top(\theta_{X_e},\psi_{X_e}) = 0$, we can design $\Theta_d = \begin{bmatrix}0 & -\theta_{X_e} & \psi_{X_e}-\pi\end{bmatrix}^\top$.

2) For $\tau_d \neq 0$: For this case, similarly, we have

$$\dot{V} = \begin{bmatrix}\hat{y}_1\\ \hat{y}_2\\ \tau^*_{d_1}\\ \hat{y}_3\\ \hat{y}_4\\ \tau_{d_2}\end{bmatrix}^\top \underbrace{\begin{bmatrix}-Q_1 & \frac{S_1^\top}{2} & & & & \\ \frac{S_1}{2} & -Q_2 & \frac{S_2^\top}{2} & & & \\ & \frac{S_2}{2} & & & & \\ & & & -Q_3 & \frac{S_3^\top}{2} & \\ & & & \frac{S_3}{2} & -Q_4 & \frac{S_4^\top}{2} \\ & & & & \frac{S_4}{2} & \end{bmatrix}}_{\Pi} \begin{bmatrix}\hat{y}_1\\ \hat{y}_2\\ \tau^*_{d_1}\\ \hat{y}_3\\ \hat{y}_4\\ \tau_{d_2}\end{bmatrix}$$

where the blank block in Π denotes the zero matrix with appropriate dimensions. If the disturbance weight S_2, S_4 satisfies $\Pi \prec 0$, then the system is asymptotically stable under the same condition of Proposition 2. If S_2, S_4 are available, then it is easy to solve Q_1, Q_2, Q_3, Q_4 satisfying $\Pi \prec 0$. If S_2, S_4 are unknown, we can obtain the L_2-gain from τ_d to the output Y such that

$$G(Y, \begin{bmatrix}\tau^*_{d_1}\\ \tau_{d_2}\end{bmatrix}) \leq \max\left(\frac{S_1}{Q_1}, \frac{|S_2|}{Q_2}, \frac{\sqrt{\bar{\lambda}_{S_3 S_3^\top}}}{\underline{\lambda}_{Q_3}}, \frac{\sqrt{\bar{\lambda}_{S_4 S_4^\top}}}{\underline{\lambda}_{Q_4}}\right) \quad (12)$$

D. Assigning Concave Passivity

According to (12), we know that the larger Q_i will lead to a smaller L_2-gain and the better transient speed. However, the larger Q_i requires sufficient large control effort as shown in (10), which is not guaranteed since the actuator's saturation exists. Thus, we introduce the concave output strict passivity by designing each Q_i as a concave factor or concave factor matrix. In order to clarify the difference, we define Q_i^c as a concave factor (matrix), such that we design $\frac{\mathrm{d}Q_i^c}{\mathrm{d}V_i} \prec 0$. Taking Q_4^c as an example, using the proposed slider-like concave factor function, we design $Q_4^c := \mathrm{diag}(\frac{\beta_1^1 k^1_{min} V_4 + \beta_2^1 k^1_{max}}{\beta_1^1 V_4 + \beta_2^1}, \frac{\beta_1^2 k^2_{min} V_4 + \beta_2^2 k^2_{max}}{\beta_1^2 V_4 + \beta_2^2}, \frac{\beta_1^3 k^3_{min} V_4 + \beta_2^3 k^3_{max}}{\beta_1^3 V_4 + \beta_2^3})$ where the associated parameters satisfy the condition of the concave factor function. Then, we have $\underline{Q}_4^c \leq Q_4^c \leq \bar{Q}_4^c$ with $\underline{Q}_4^c = \mathrm{diag}(k^1_{min}, k^2_{min}, k^3_{min})$ and $\bar{Q}_4^c = \mathrm{diag}(k^1_{max}, k^2_{max}, k^3_{max})$. Therefore, as V_4 converges to zero, Q_4^c increases, such that the associated L_2-gain of the passive subsystem Σ_4^p decreases. $\underline{Q}_4^c$ should be sufficient small to handle the input saturation and $\bar{Q}_4^c$ is sufficient large to guarantee the control performance. The other Q_i^c follows the same guidance. With desired Q_i^c, we can achieve good control performance even when $\dot{X}_{ref}$ and $\dot{\Theta}_d$ are unavailable.

V. Numerical Simulation

This section demonstrates the effectiveness of the feedback concavification concept and the proposed architecture of the interconnected passive systems in the application of the underactuated AUVs compared with a PD controller used in [12]–[14]. All the simulation files of this paper are available at the link[1]. The detailed model parameters of *Hippocampus* are published and available at [20]. The reference trajectory is infinity-shaped as $X_{ref}(t) = \begin{bmatrix}a_x \sin(\frac{\pi}{15}t) & a_y(\frac{\pi}{30}t) & 0.1t\end{bmatrix}^\top$. To evaluate the robustness, the disturbance is selected as $\tau_d = [0.2\sin(0.1t+1), 0.1\sin(0.15t+0.9), 0.1\sin(0.1t+0.5), 0.1\sin(0.05t+1), 0.1\sin(0.1t+2), 0.1\sin(0.15t+3)]^\top$. The parameters of the passive controller is designed as $Q_1 = 8$, $Q_2 = 10$, $Q_3 = \mathrm{diag}(0.01, 5, 8)$, $Q_4 = \mathrm{diag}(0.001, 0.1, 0.1)$. We select the slider-like concave factor to assign the concavity for the concave passive controller where the parameter $\alpha = 1$. The parameters of the the concave passive controller is designed as: $Q_1^c = \frac{8V_1+0.5}{V_1+0.01}$, $Q_2^c = \frac{10V_2+1.6}{V_2+0.02}$, $Q_3^c = \mathrm{diag}(\frac{0.01V_3+1}{V_3+1}, \frac{5V_3+0.2}{V_3+0.01}, \frac{8V_3+0.6}{V_3+0.02})$, $Q_4^c = \mathrm{diag}(\frac{0.001V_4+0.01}{V_4+1}, \frac{0.001V_4+0.2}{0.01V_4+0.02}, \frac{0.001V_4+0.2}{0.01V_4+0.02})$.

For a fair comparison, all the parameters of the above controller are well-tuned under the reference trajectory with $a_x = 4, a_y = 8$ when $\tau_d = 0$. Moreover, the limit of each motor is defined as $\bar{\mathcal{T}}_i = 3$. For $\tau_d = 0$, the tracking results are shown in Fig.4 and Fig.5. When $\tau_d = 0$, all controllers perform well. From Fig.5, we can find that the passive controller outperforms the PD controller, and the feedback concavification techniques can improve the tracking performance and reduce the tracking error under the input saturation.

Fig.6 and Fig.7 display the simulation results with $\tau_d \neq 0$. From Fig.6, we can observe that the PD controller becomes invalid when the disturbance is considering. However, the passive controller consistently demonstrates reliable performance. It is evident that the feedback concavification techniques can significantly enhance tracking performance and robustness.

Remark 1. *We compared the controllers with different reference trajectories with different a_x, a_y. From those results, the concave passive controller consistently outperforms the other controllers. Nevertheless, sometimes, the PD controller becomes invalid when we change the reference. The adaptability and robustness of the concave passive controller are evident. One can check with the provided files at https://github.com/shuyuanfan/Hippocampus-Concavity.git.*

VI. Conclusion

The paper introduces a novel approach for controlling underactuated Autonomous Underwater Vehicles (AUVs) using feedback concavification based on the passivity theorem. With the help of the Euclidean vector, an interconnected passive architecture of the 6-DOF underactuated AUV is proposed, simplifying the analysis and the assignment of closed-loop behavior. Simulation results effectively illustrate the effectiveness of this proposed passive structure for AUV control. After introducing the concavity, the control performance experiences a significant enhancement. The authors plan to further explore the potential of feedback concavification in other scenarios.

[1] https://github.com/shuyuanfan/Hippocampus-Concavity.git

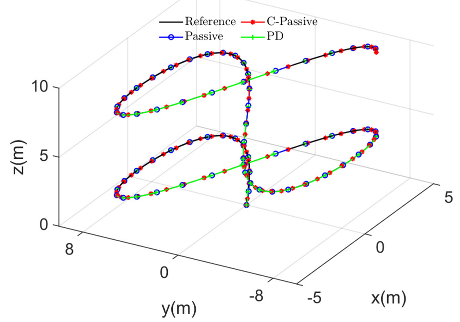

Fig. 4. Tracking results without disturbance where 'C-Passive' denotes the concave passive controller

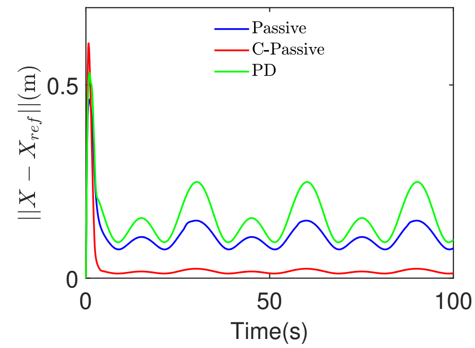

Fig. 5. Results of tracking error without disturbance

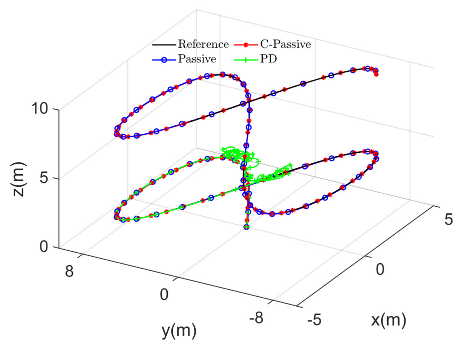

Fig. 6. Tracking results with disturbance

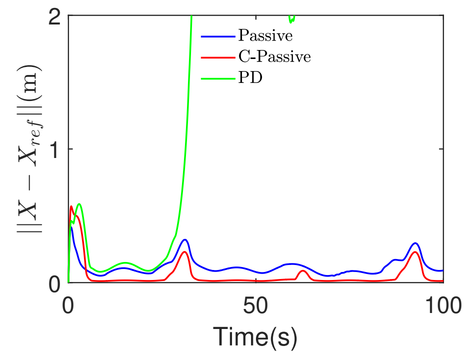

Fig. 7. Results of tracking error with disturbance

REFERENCES

[1] M. J. Er, H. Gong, Y. Liu, and T. Liu, "Intelligent trajectory tracking and formation control of underactuated autonomous underwater vehicles: A critical review," *IEEE Transactions on Systems, Man, and Cybernetics: Systems*, 2023.

[2] L. Hong, R. Fang, X. Cai, and X. Wang, "Numerical investigation on hydrodynamic performance of a portable auv," *Journal of Marine Science and Engineering*, vol. 9, no. 8, p. 812, 2021.

[3] T. I. Fossen, *Handbook of marine craft hydrodynamics and motion control*. John Wiley & Sons, 2011.

[4] K. D. Do and J. Pan, *Control of ships and underwater vehicles: design for underactuated and nonlinear marine systems*. Springer, 2009, vol. 1.

[5] S. Bhat and I. Stenius, "Hydrobatics: A review of trends, challenges and opportunities for efficient and agile underactuated auvs," in *2018 IEEE/OES Autonomous Underwater Vehicle Workshop (AUV)*, 2018, pp. 1–8.

[6] F. Muñoz, J. S. Cervantes-Rojas, J. M. Valdovinos, O. Sandre-Hernández, S. Salazar, and H. Romero, "Dynamic neural network-based adaptive tracking control for an autonomous underwater vehicle subject to modeling and parametric uncertainties," *Applied Sciences*, vol. 11, no. 6, p. 2797, 2021.

[7] C. Wang, W. Cai, J. Lu, X. Ding, and J. Yang, "Design, modeling, control, and experiments for multiple auvs formation," *IEEE Transactions on Automation Science and Engineering*, vol. 19, no. 4, pp. 2776–2787, 2022.

[8] T. Elmokadem, M. Zribi, and K. Youcef-Toumi, "Trajectory tracking sliding mode control of underactuated auvs," *Nonlinear Dynamics*, vol. 84, pp. 1079–1091, 2016.

[9] A. Wadi, S. Mukhopadhyay, and J.-H. Lee, "A novel disturbance-robust adaptive trajectory tracking controller for a class of underactuated autonomous underwater vehicles," *Ocean Engineering*, vol. 189, p. 106377, 2019.

[10] T. Elmokadem, M. Zribi, and K. Youcef-Toumi, "Terminal sliding mode control for the trajectory tracking of underactuated autonomous underwater vehicles," *Ocean Engineering*, vol. 129, pp. 613–625, 2017.

[11] A. Hackbarth, E. Kreuzer, and E. Solowjow, "Hippocampus: A micro underwater vehicle for swarm applications," in *2015 IEEE/RSJ International Conference on Intelligent Robots and Systems (IROS)*, 2015, pp. 2258–2263.

[12] D. A. Duecker, A. Hackbarth, T. Johannink, E. Kreuzer, and E. Solowjow, "Micro underwater vehicle hydrobatics: A submerged furuta pendulum," in *2018 IEEE International Conference on Robotics and Automation (ICRA)*, 2018, pp. 7498–7503.

[13] K. Yao, N. Bauschmann, T. L. Alff, W. Cheah, D. A. Duecker, K. Groves, O. Marjanovic, and S. Watson, "Image-based visual servoing switchable leader-follower control of heterogeneous multi-agent underwater robot system," in *2023 IEEE International Conference on Robotics and Automation (ICRA)*. IEEE, 2023, pp. 5200–5206.

[14] D. A. Duecker, C. Horst, and E. Kreuzer, "From aerobatics to hydrobatics: Agile trajectory planning and tracking for micro underwater robots," in *2021 IEEE/RSJ International Conference on Intelligent Robots and Systems (IROS)*. IEEE, 2021, pp. 8617–8624.

[15] J. C. Willems, "Dissipative dynamical systems part i: General theory," *Archive for rational mechanics and analysis*, vol. 45, no. 5, pp. 321–351, 1972.

[16] R. Sepulchre, M. Jankovic, and P. V. Kokotovic, *Constructive nonlinear control*. Springer Science & Business Media, 2012.

[17] B. Brogliato, R. Lozano, B. Maschke, O. Egeland *et al.*, "Dissipative systems analysis and control," *Theory and Applications*, vol. 2, pp. 2–5, 2007.

[18] A. Van der Schaft, *L2-gain and passivity techniques in nonlinear control, 3rd ed.* Springer, 2016.

[19] J. W. Simpson-Porco, "Equilibrium-independent dissipativity with quadratic supply rates," *IEEE Transactions on Automatic Control*, vol. 64, no. 4, pp. 1440–1455, 2019.

[20] D. A. Duecker, E. Kreuzer, G. Maerker, and E. Solowjow, "Parameter identification for micro underwater vehicles," *PAMM*, vol. 18, no. 1, p. e201800350, 2018.